nature biotechnology

Tumor refractoriness to anti-VEGF treatment is mediated by CD11b$^+$Gr1$^+$ myeloid cells

Farbod Shojaei[1], Xiumin Wu[1], Ajay K Malik[1], Cuiling Zhong[1], Megan E Baldwin[1], Stefanie Schanz[1], Germaine Fuh[1], Hans-Peter Gerber[1,2] & Napoleone Ferrara[1]

Vascular endothelial growth factor (VEGF) is an essential regulator of normal and abnormal blood vessel growth. A monoclonal antibody (mAb) that targets VEGF suppresses tumor growth in murine cancer models and human patients. We investigated cellular and molecular events that mediate refractoriness of tumors to anti-angiogenic therapy. Inherent anti-VEGF refractoriness is associated with infiltration of the tumor tissue by CD11b$^+$Gr1$^+$ myeloid cells. Recruitment of these myeloid cells is also sufficient to confer refractoriness. Combining anti-VEGF treatment with a mAb that targets myeloid cells inhibits growth of refractory tumors more effectively than anti-VEGF alone. Gene expression analysis in CD11b$^+$Gr1$^+$ cells isolated from the bone marrow of mice bearing refractory tumors reveals higher expression of a distinct set of genes known to be implicated in active mobilization and recruitment of myeloid cells. These findings indicate that, in our models, refractoriness to anti-VEGF treatment is determined by the ability of tumors to prime and recruit CD11b$^+$Gr1$^+$ cells.

The ability of therapeutic agents to inhibit tumor growth is frequently limited by the development of resistance. Several mechanisms of intrinsic refractoriness or resistance to various cytotoxic agents have been identified in tumor cells[1]. There is growing evidence that host stromal–tumor cell interactions play an important role in tumor growth, as stromal cells may secrete a variety of angiogenic factors. In addition, the view that stromal cells are genetically stable has recently been challenged[2,3]. Therefore, stromal–tumor cell interactions might contribute to both inherent refractoriness and acquired resistance to anti-angiogenic treatments.

VEGF-A is a well-characterized regulator of angiogenesis and several anti-VEGF strategies have been implemented[4,5]. VEGF-A blockade using the humanized anti-VEGF-A monoclonal antibody (mAb) bevacizumab (Avastin) or its murine precursor significantly inhibited angiogenesis and growth of human tumor xenografts[6]. However, the degree of inhibition varied among different tumor cell lines. Furthermore, the effects were most pronounced when the treatment was started at early stages of tumor growth. The molecular and cellular events underlying refractoriness or resistance to anti-VEGF are incompletely understood[6]. Tumor cell–intrinsic or treatment-induced expression of alternative pro-angiogenic factors during tumor progression might be implicated[7,8]. There is considerable debate regarding the nature of the cell types involved. Tumor-infiltrating fibroblasts[9] and various pro-inflammatory cells have been reported to secrete factors that promote endothelial cell migration and survival[10].

Here, we conducted a series of studies to elucidate the role of myeloid cells in responsiveness to anti-VEGF therapy. We found that priming and recruitment of CD11b$^+$Gr1$^+$ myeloid cells in some tumor models represents a cellular mechanism that mediates refractoriness to anti-VEGF treatment. We also show that anti-VEGF therapy in combination with a mAb that targets CD11b$^+$Gr1$^+$ myeloid cells partially overcomes refractoriness.

RESULTS

Recruitment of BMMNCs by refractory tumors

We screened several murine tumor cell lines, known to be syngeneic/poorly immunogenic in C57BL/6 mice, to identify high and low responders to an anti-VEGF mAb (hereafter anti-VEGF). The cell lines we chose are derived from a melanoma (B16F1)[11], two lymphomas (EL4 (ref. 12) and TIB6 (ref. 13)) and a lung carcinoma (Lewis Lung Carcinoma, LLC)[14].

To test the hypothesis that responsiveness to anti-VEGF may be related to tumor recruitment of bone marrow mononuclear cells (BMMNCs), we reconstituted the hematopoietic system in lethally irradiated C57BL/6 mice with green fluorescent protein (GFP)–expressing BMMNCs[15]. Next, GFP$^+$ chimeric mice were implanted with tumor cell lines. The growth of TIB6 and B16F1 tumors was markedly inhibited by anti-VEGF in GFP$^+$ chimeric mice (**Fig. 1a**). In contrast, the growth of LLC and EL4 tumors was only modestly and transiently inhibited. Several independent experiments performed in both chimeric and non-chimeric mice yielded similar results (**Supplementary Fig. 1** online). At day 14 after inoculation, compared to the control mAb (hereafter control), anti-VEGF treatment inhibited tumor growth in TIB6 and B16F1 tumors by 78.3% ± 1.7 ($n = 2$ experiments) and 73.94% ± 11.08 ($n = 7$), respectively. Growth of EL4 and LLC tumors was inhibited 32.4% ± 10.6 ($n = 6$) and 29.6% ± 6.1 ($n = 9$), respectively. Therefore, we define TIB6 and B16F1

[1]Genentech, Inc., 1 DNA Way, S. San Francisco, California 94080, USA. [2]Present address: Seattle Genetics Inc., 21823 30th Drive, SE, Bothell, Washington 98021, USA. Correspondence should be addressed to F.S. (farbod@gene.com) or N.F. (nf@gene.com).

Received 8 March; accepted 3 July; published online 29 July 2007; doi:10.1038/nbt1323

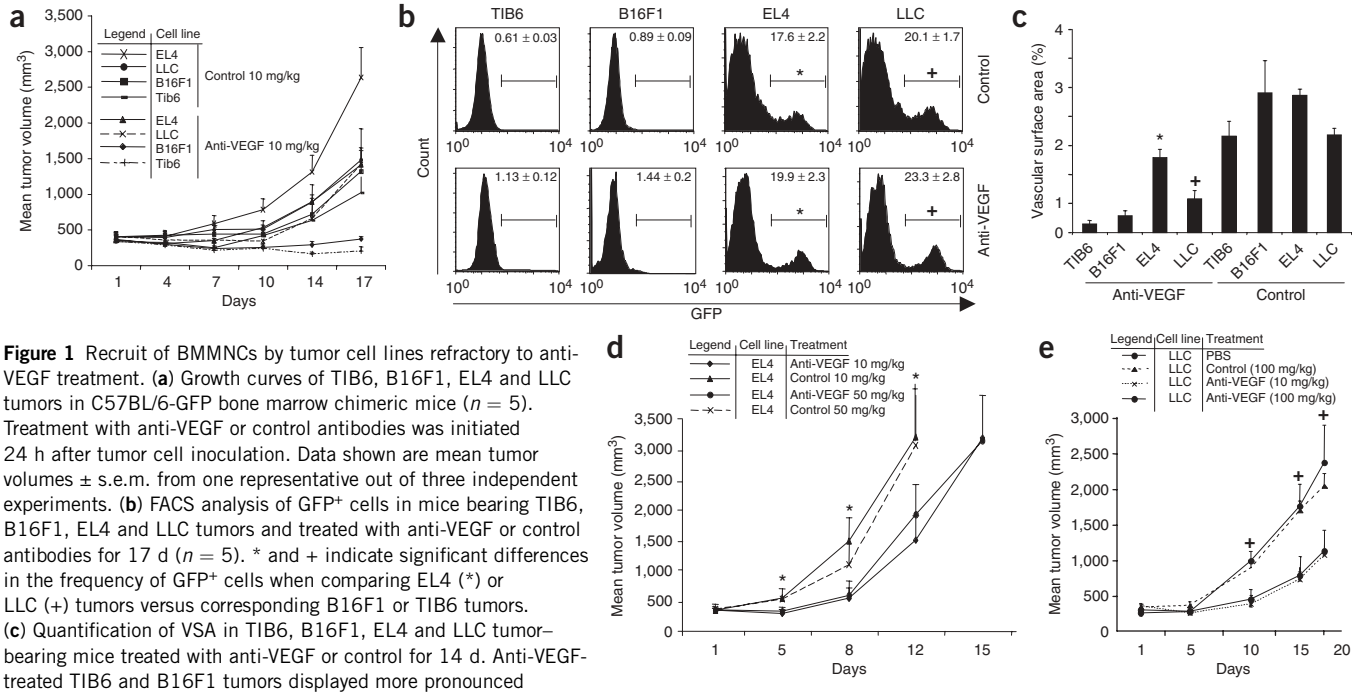

Figure 1 Recruit of BMMNCs by tumor cell lines refractory to anti-VEGF treatment. (**a**) Growth curves of TIB6, B16F1, EL4 and LLC tumors in C57BL/6-GFP bone marrow chimeric mice ($n = 5$). Treatment with anti-VEGF or control antibodies was initiated 24 h after tumor cell inoculation. Data shown are mean tumor volumes ± s.e.m. from one representative out of three independent experiments. (**b**) FACS analysis of GFP$^+$ cells in mice bearing TIB6, B16F1, EL4 and LLC tumors and treated with anti-VEGF or control antibodies for 17 d ($n = 5$). * and + indicate significant differences in the frequency of GFP$^+$ cells when comparing EL4 (*) or LLC (+) tumors versus corresponding B16F1 or TIB6 tumors. (**c**) Quantification of VSA in TIB6, B16F1, EL4 and LLC tumor–bearing mice treated with anti-VEGF or control for 14 d. Anti-VEGF-treated TIB6 and B16F1 tumors displayed more pronounced reductions in VSA than LLC or EL4 tumors. Data shown are means ± s.e.m. of values from 9–15 sections of 3–5 tumors per treatment group. (**d**) Growth of EL4 tumors in beige nude XID mice ($n = 10$) treated with control (10 and 50 mg/kg, intraperitoneally (IP), twice weekly) or anti-VEGF (10 and 50 mg/kg, IP, twice weekly). Treatment was initiated 24 h after tumor cell inoculation. (**e**) Growth of LLC tumors ($n = 10$) in beige nude XID mice as described in **b**. Anti-VEGF (10 and 100 mg/kg) and control antibodies (100 mg/kg) were administered IP, twice weekly, respectively. * indicates that tumors from EL4 tumor–bearing mice are significantly different ($P < 0.05$) from B16F1 and TIB6 tumors. + indicates a significant difference ($P < 0.05$) between LLC tumor–bearing mice treated with anti-VEGF or control (where applicable) and similarly treated B16F1 and TIB6 animals.

tumors as sensitive to anti-VEGF therapy (hereafter 'sensitive'), and EL4 and LLC tumors as refractory (hereafter 'refractory') to such treatment.

Tumor isolates from refractory tumors had an increased ($P < 0.05$) frequency of GFP$^+$ bone marrow cells in both anti-VEGF– and control-treated mice compared to isolates from sensitive ones (**Fig. 1b**), suggesting that refractoriness to anti-VEGF might be associated with the recruitment of BMMNCs. It has been previously proposed that bone marrow cells, including endothelial progenitor cells[16] and myeloid cells[17], are incorporated in the tumor vasculature. To determine whether BMMNCs directly contribute to the vasculature in our models, we stained tumor sections with CD31 (PECAM) and GFP (**Supplementary Fig. 2** online). On day 14 of treatment, and irrespective of the tumor type, the vast majority of CD31$^+$ vascular structures in anti-VEGF– or control-treated tumors were devoid of GFP expression (**Supplementary Fig. 2**; and data not shown). These findings suggest that BMMNCs do not significantly contribute to tumor vasculature in our models. Vascular surface areas (VSA) were significantly increased in refractory tumors compared to sensitive ones (**Fig. 1c**), suggesting that refractoriness is mediated by the development of a neovascular supply.

To test the possibility that the immune system may affect such refractoriness, we implanted LLC or EL4 cells in beige nude X-linked immunodeficient (XID) mice. The growth inhibition induced by anti-VEGF was similar to that observed in immunocompetent mice (**Fig. 1d,e**). Conversely, B16F1 and TIB6 tumors were responsive to anti-VEGF treatment in immunodeficient mice (data not shown). We also tested whether doses of anti-VEGF five- or tenfold higher than those routinely administered achieved greater tumor growth inhibition. However, the effects of higher doses of anti-VEGF were indistinguishable from those of the lower dose (**Fig. 1d,e**). Thus, refractoriness to anti-VEGF is T-cell– and B-cell–independent and is not caused by suboptimal dosing.

Importance of priming and recruitment of BMMNCs

We performed admixing experiments (**Supplementary Fig. 3** online) with B16F1 tumors because they are of nonhematopoietic origin and are sensitive to anti-VEGF. GFP$^+$ cells were isolated from tumors (**Fig. 2a**) or the bone marrow (**Fig. 2b**) of chimeric mice implanted with refractory or sensitive tumors. Fluorescence-activated cell sorting (FACS) analysis documented the purity of GFP$^+$ cells in each compartment.

Admixing B16F1 with BMMNCs primed by refractory tumors resulted in significant ($P < 0.05$) growth stimulation (**Fig. 2c,d**). In contrast, growth rates of B16F1 tumors were not significantly affected by admixing with BMMNCs primed by B16F1 tumors or control Matrigel implants (**Fig. 2c,d**). Therefore, GFP$^+$ cells from EL4 and LLC tumors mediated refractoriness to anti-VEGF when admixed with B16F1 tumors (**Fig. 2e,f**). However, GFP$^+$ BMMNCs, when implanted alone, did not give rise to tumors, demonstrating the lack of contaminating tumor cells (data not shown). We conclude that physical proximity between BMMNCs and sensitive tumors is insufficient to induce refractoriness and priming, or 'instruction' of bone marrow cells by refractory tumors appears to be a key step in the establishment of VEGF-independent tumor growth.

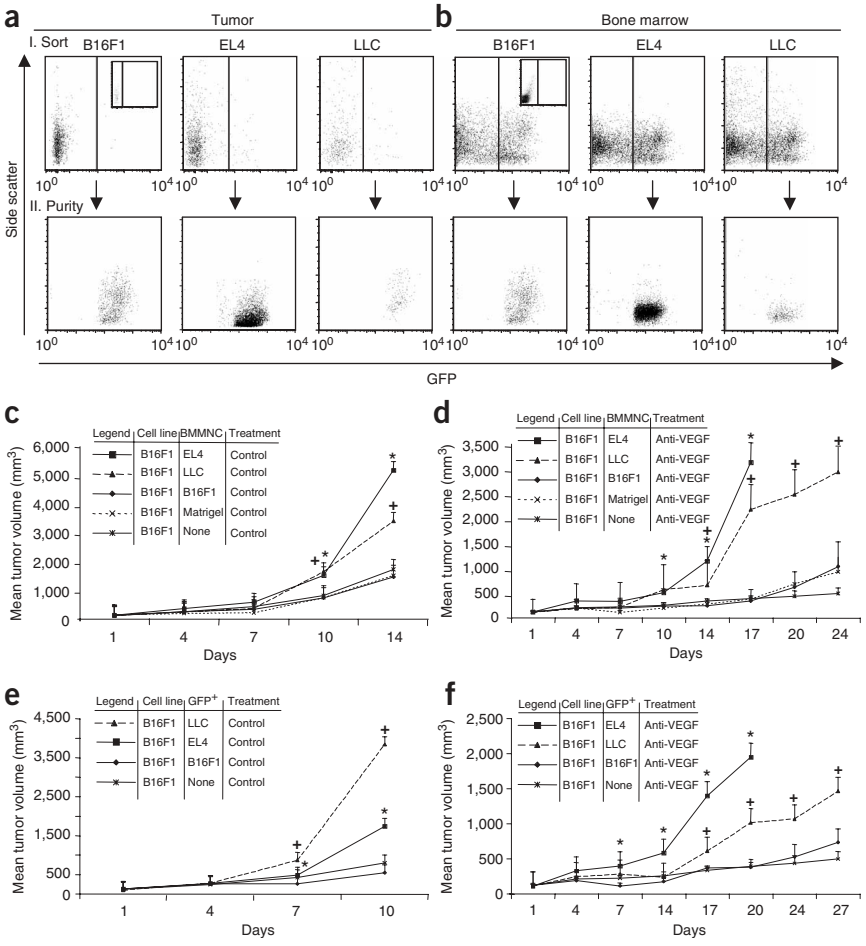

Figure 2 BMMNCs and tumor associated-GFP$^+$ cells from mice bearing EL4 and LLC tumors contribute to refractoriness to anti-VEGF treatment. (**a**,**b**) Using FACS sorting, GFP$^+$ cells were isolated from tumors (**a**) and BMMNCs (**b**) of implanted mice. The purity of the GFP$^+$ cells was confirmed in post-sort analysis. (**c**) Growth of 2.5×10^6 B16F1 tumor cells when admixed with 10^6 BMMNCs isolated from EL4, LLC or B16F1 tumor-bearing mice and treated with control. BMMNCs from matrigel-implanted or from naïve mice served as controls in the admixing experiments ($n = 5$) (**d**) Growth curves of B16F1 tumors admixed with GFP$^+$ BMMNCs isolated from EL4, LLC or B16F1 tumor–bearing mice and treated with anti-VEGF. GFP$^+$ bone marrow cells from EL4 and LLC (but not B16F1) tumor–bearing mice significantly increased the growth of B16F1 tumors ($n = 4$). Data shown in **a** and **b** are from one representative out of at least two independent experiments. (**e**,**f**) Growth of 2×10^6 B16F1 tumors admixed with 5×10^5 GFP$^+$ cells isolated from 14-d-old EL4, LLC or B16F1 tumors treated either with control (**e**) or anti-VEGF (**f**). * and + denote significant difference ($P < 0.05$) in tumor volume in admixing experiments using GFP$^+$ cells isolated from bone marrow or tumors in mice primed with EL4 (*) or LLC (+) tumors compared to B16F1 cells alone or admixed with GFP$^+$ cells isolated from matrigel or B16F1 primed mice.

CD11b$^+$Gr1$^+$ cells mediate refractoriness to anti-VEGF

BMMNCs comprise a heterogeneous population including cells of primitive, myeloid and lymphoid lineages[18]. Therefore, we sought to determine which subset(s) of BMMNCs plays the major role in mediating refractoriness to anti-VEGF. Our initial observations (**Fig. 3a–d**) suggested that CD11b$^+$Gr1$^+$ cells, representing a subset of the myeloid population[19], are primarily responsible for such refractoriness. To further test this hypothesis, we performed *in vitro* cell migration assays to examine the effects of soluble extracts (conditioned media) from refractory or sensitive tumors on BMMNC migration. We found greater ($P < 0.05$) migration of bone marrow CD11b$^+$Gr1$^+$ cells toward the soluble extracts of refractory compared to sensitive tumors (**Fig. 3a**). This migration was unaffected by anti-VEGF (10 μg/ml) in the medium, suggesting that myeloid cell recruitment is tumor-intrinsic, VEGF-independent and is not induced by the treatment. These results are consistent with the finding that anti-VEGF treatment did not block BMMNCs homing into refractory tumors (**Fig. 1b**).

Flow cytometric analysis of infiltrating BMMNCs from refractory tumor isolates demonstrated a significant ($P < 0.05$) enrichment in CD11b$^+$Gr1$^+$cells compared to sensitive tumors (**Fig. 3b** and **Supplementary Fig. 4a** online). Furthermore, we found a higher percentage ($P < 0.05$) of CD11b$^+$Gr1$^+$ cells in the bone marrow of mice bearing refractory tumors (**Fig. 3c** and **Supplementary Fig. 4b**).

In addition to CD11b and Gr1, kinetics of other hematopoietic lineages were investigated (**Supplementary Fig. 5** online). A significant reduction ($P < 0.05$) in the frequency of B-lymphoid cells and dendritic cells was notable in refractory tumors (**Supplementary Fig. 5a**). In addition, we found a reduction in the frequency of B- and T-lymphoid and dendritic cells in the bone marrow of mice bearing refractory tumors compared to bone marrow from mice with sensitive tumors (**Supplementary Fig. 5b**). Thus, the increase in the frequency of myeloid cells in refractory tumors may be associated with a reduction in other hematopoietic lineages.

Because previous studies suggested that splenic CD11b$^+$Gr1$^+$cells contribute to tumor expansion[20,21], we also examined the spleens of tumor-bearing mice. In agreement with the findings in bone marrow and tumors, we found an increase ($P < 0.05$) in the frequency of CD11b$^+$Gr1$^+$ cells in spleens and enlarged spleen sizes ($P < 0.05$) in mice implanted with refractory tumors compared to sensitive ones (**Supplementary Fig. 6a**,**b** online).

To directly test the ability of myeloid cells to mediate refractoriness to anti-VEGF, we isolated CD11b$^+$Gr1$^+$ and CD11b$^-$Gr1$^-$ subpopulations (**Supplementary Fig. 7** online) from the bone marrow of mice primed with refractory or sensitive tumors and admixed them with B16F1 tumor cells. In these experiments, we used non-chimeric C57Bl6 mice, because we had already established the contribution of BMMNCs in the chimeric model. CD11b$^+$Gr1$^+$ (but not CD11b$^-$Gr1$^-$) cells primed by refractory tumors promoted refractoriness (**Fig. 3d**). In contrast, CD11b$^+$Gr1$^+$ cells primed by sensitive tumors failed to induce refractoriness (**Supplementary Fig. 8a** online). Additionally, tumor-associated CD11b$^+$Gr1$^+$ cells isolated from refractory tumors were able to confer refractoriness to sensitive tumors (**Fig. 3e**,**f**).

We quantified the VSA in B16F1 tumors admixed with bone marrow CD11b$^+$Gr1$^+$ or CD11b-Gr1- cells to test whether CD11b$^+$Gr1$^+$ cells have any effects on tumor angiogenesis

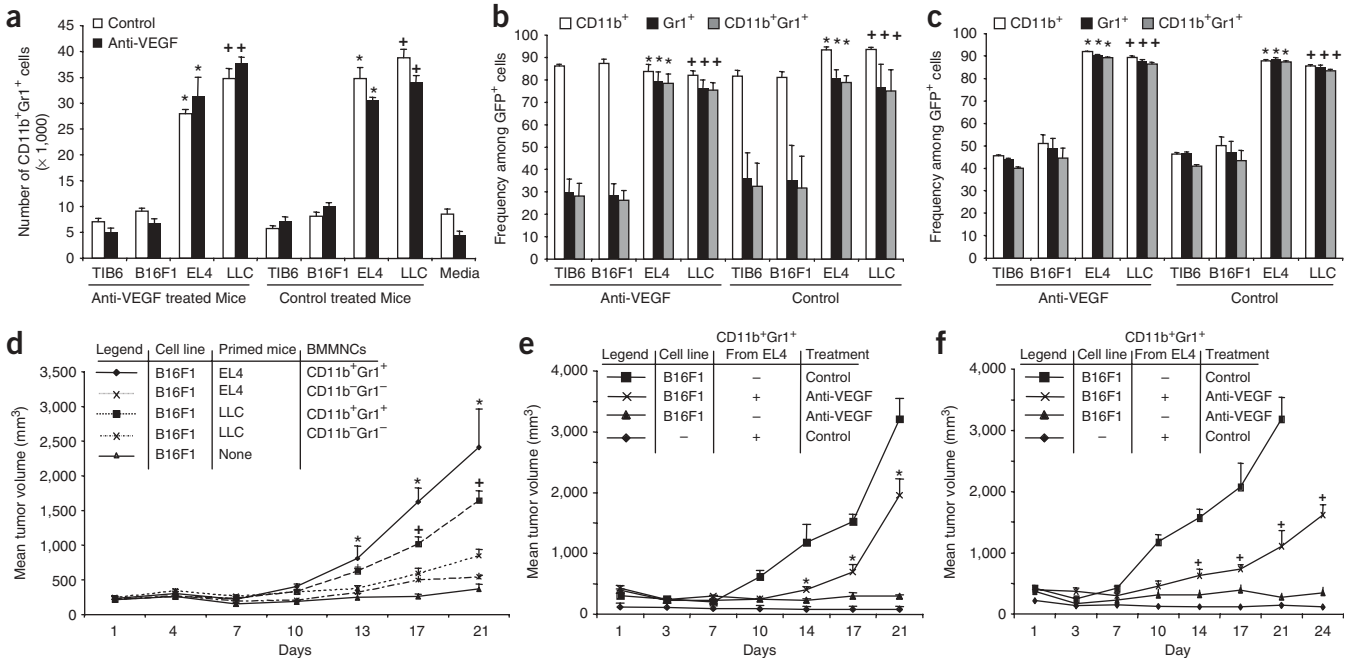

Figure 3 CD11b$^+$Gr1$^+$ cells isolated from mice bearing refractory tumors are a major hematopoietic cell population mediating refractoriness to anti-VEGF treatment. (**a**) Numbers of migrated CD11b$^+$Gr1$^+$ cells from freshly isolated BMMNCs after exposure to soluble extracts from control or anti-VEGF-treated TIB6, B16F1, EL4 and LLC tumors. Refractory tumors induce VEGF-independent migration of bone marrow myeloid cells. (**b**) Multi-lineage analysis of tumor isolates from mice implanted with TIB6, B16F1, EL4 and LLC tumors and treated with control or anti-VEGF antibodies. EL4 and LLC, but not TIB6 or B16F1 tumors, displayed a significant increase in the frequency of tumor associated CD11b$^+$Gr1$^+$ cells. Data shown are from one representative out of two independent experiments. (**c**) Multi-lineage analysis of BMMNCs in mice implanted with TIB6, B16F1, EL4 and LLC tumors. Consistent with the data obtained in tumor isolates (**Fig. 3b**), there was a significant ($P < 0.05$) increase in the frequency of CD11b$^+$Gr1$^+$cells in the bone marrow of anti-VEGF-refractory tumor–bearing mice. Data shown are from one representative out of two independent experiments. (**d**) Bone marrow CD11b$^+$Gr1$^+$cells play a key role in mediating resistance to anti-VEGF treatment. Growth curves of B16F1 tumors admixed with EL4- and LLC-primed, bone marrow CD11b$^+$Gr1$^+$cells and treated with anti-VEGF ($n = 5$ per group). Data shown are from one representative of two independent experiments. (**e**,**f**) Growth curves of B16F1 cells admixed with tumor-associated CD11b$^+$Gr1$^+$ cells isolated from EL4 (**e**) and LLC (**f**) tumor–bearing mice. For admixing experiment, 3×10^5 FACS sorted CD11b$^+$Gr1$^+$ cells isolated from EL4 or LLC tumor–bearing mice and were admixed with 3×10^6 B16F1 cells and were implanted in C57BL/6 mice ($n = 5$). * and + denote significant difference ($P < 0.05$) in tumor volume in the admixing experiments using CD11b$^+$Gr1$^+$ cells isolated from bone marrow or tumors of mice primed with EL4 (*) or LLC (+) tumors compared to B16F1 tumors alone or admixed with CD11b-Gr1- cells.

(**Supplementary Fig. 8b**). The VSA in the CD11b$^+$Gr1$^+$ admixture was significantly ($P < 0.05$) greater than B16F1 alone or the admixture with CD11b-Gr1- cells, indicating that CD11b$^+$Gr1$^+$ cells promote new vessel growth, even in the presence of anti-VEGF. Therefore, both bone marrow– and tumor-associated CD11b$^+$Gr1$^+$ cells are sufficient to confer refractoriness to anti-VEGF.

Effects of combination therapy on growth in refractory tumors

To corroborate our findings implicating myeloid cells in refractoriness to anti-VEGF, we aimed at reducing the numbers of Gr1$^+$ myeloid cells in the peripheral blood, by using an anti-Gr1 mAb (hereafter, anti-Gr1)[22]. Anti-Gr1 was tested alone or in combination with anti-VEGF in mice implanted with EL4 (**Fig. 4a**,**b**) or LLC tumors (**Fig. 4c**,**d**). When administered alone, anti-Gr1 treatment significantly ($P < 0.05$) reduced the numbers of Gr1$^+$ cells in the peripheral blood and in the tumors, but did not affect tumor growth and vascularization of either EL4 or LLC tumors (**Fig. 4a–d**). However, combination treatment (anti-VEGF and anti-Gr1) resulted in a significant difference ($P < 0.05$) in terminal weight and volume in EL4 (**Fig. 4b**) and LLC tumors (**Fig. 4d**) relative to anti-VEGF alone. FACS analysis of EL4 (**Fig. 4b**) and LLC tumor-bearing animals (**Fig. 4d**) revealed a significant ($P < 0.05$) reduction in Gr1$^+$ myeloid cells in the peripheral blood. In the combination treatment group, immunohistochemical (IHC) analysis indicated a reduction in tumor VSA, which correlated with a reduction in tumor growth rates (**Fig. 4c**,**d**). Therefore, one of the possible mechanisms by which Gr1$^+$ cells promote tumor growth is the induction of angiogenesis. Notably, the combination treatment only reduced the amounts of CD11b$^+$Gr1$^+$ cells within EL4 and LLC tumors, indicating that targeting the Gr1$^+$ population alone may not be sufficient for complete myeloablation and thus may account for incomplete tumor growth inhibition.

Refractoriness is not mediated by PlGF or VEGF-B

To determine whether our findings can be extended to other inhibitors of the VEGF pathway, we treated mice bearing refractory or sensitive tumors with mFlt(1-3)-IgG, a high affinity chimeric soluble VEGF receptor (VEGFR)-1 variant, which neutralizes not only VEGF-A but also PlGF and VEGF-B[23,24]. The 'VEGF-Trap'[25], a blocker presently undergoing clinical development, has the same binding specificity as mFlt(1-3)-IgG. Analysis of tumor volumes in refractory tumors (**Fig. 5a**,**b**) did not reveal any significant difference in the magnitude of tumor growth inhibition in the anti-VEGF–treated mice versus the mFlt(1-3)-IgG group. Sensitive tumors (**Fig. 5c**,**d**), however, were similarly responsive to both anti-VEGF and mFlt(1-3)-IgG. Furthermore, analysis of BMMNCs (**Fig. 5e**) and tumors (**Fig. 5f**) did not

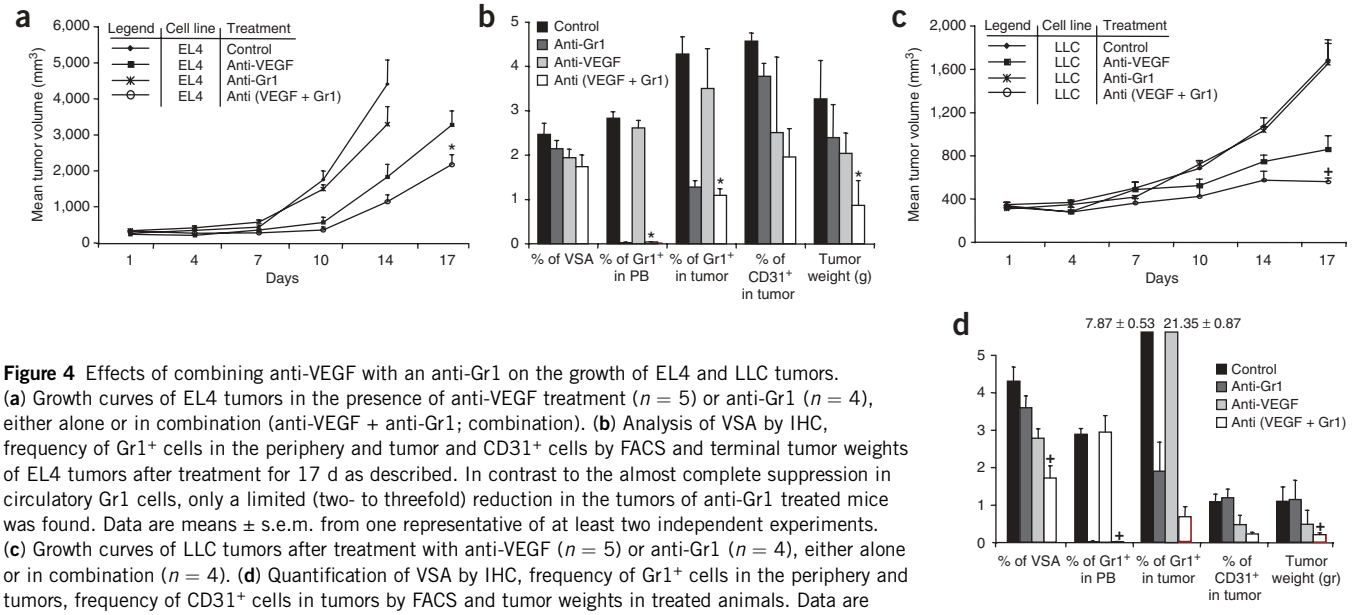

Figure 4 Effects of combining anti-VEGF with an anti-Gr1 on the growth of EL4 and LLC tumors. (**a**) Growth curves of EL4 tumors in the presence of anti-VEGF treatment ($n = 5$) or anti-Gr1 ($n = 4$), either alone or in combination (anti-VEGF + anti-Gr1; combination). (**b**) Analysis of VSA by IHC, frequency of $Gr1^+$ cells in the periphery and tumor and $CD31^+$ cells by FACS and terminal tumor weights of EL4 tumors after treatment for 17 d as described. In contrast to the almost complete suppression in circulatory Gr1 cells, only a limited (two- to threefold) reduction in the tumors of anti-Gr1 treated mice was found. Data are means ± s.e.m. from one representative of at least two independent experiments. (**c**) Growth curves of LLC tumors after treatment with anti-VEGF ($n = 5$) or anti-Gr1 ($n = 4$), either alone or in combination ($n = 4$). (**d**) Quantification of VSA by IHC, frequency of $Gr1^+$ cells in the periphery and tumors, frequency of $CD31^+$ cells in tumors by FACS and tumor weights in treated animals. Data are means ± s.e.m. from one representative of at least two independent experiments. * indicates a significant difference ($P < 0.05$) between EL4 tumor–bearing mice treated with anti-VEGF compared and combination-treated animals. **+** indicates that the means of the differences in LLC tumor–bearing mice treated with anti-VEGF compared to combination-treated mice is significant ($P < 0.05$).

show any significant difference in the numbers of bone marrow– and tumor-associated myeloid cells in sensitive or refractory tumors between the treatment groups. Therefore, although previous studies implicated VEGFR-1 in the recruitment of subsets of BMMNCs[26,27], our findings suggest that VEGFR-1 activation does not play a significant role in mediating refractoriness in our models.

Refractoriness to anti-VEGF versus cytotoxic agents

The finding that myeloid cells mediate refractoriness to anti-VEGF raises the question whether the same population also mediates resistance to other anti-cancer agents such as cytotoxic chemotherapy. To address this question, we treated tumor-bearing animals with two cytotoxic agents, 5-fluorouracil (5FU) and gemcitabine (Gamzar). EL4

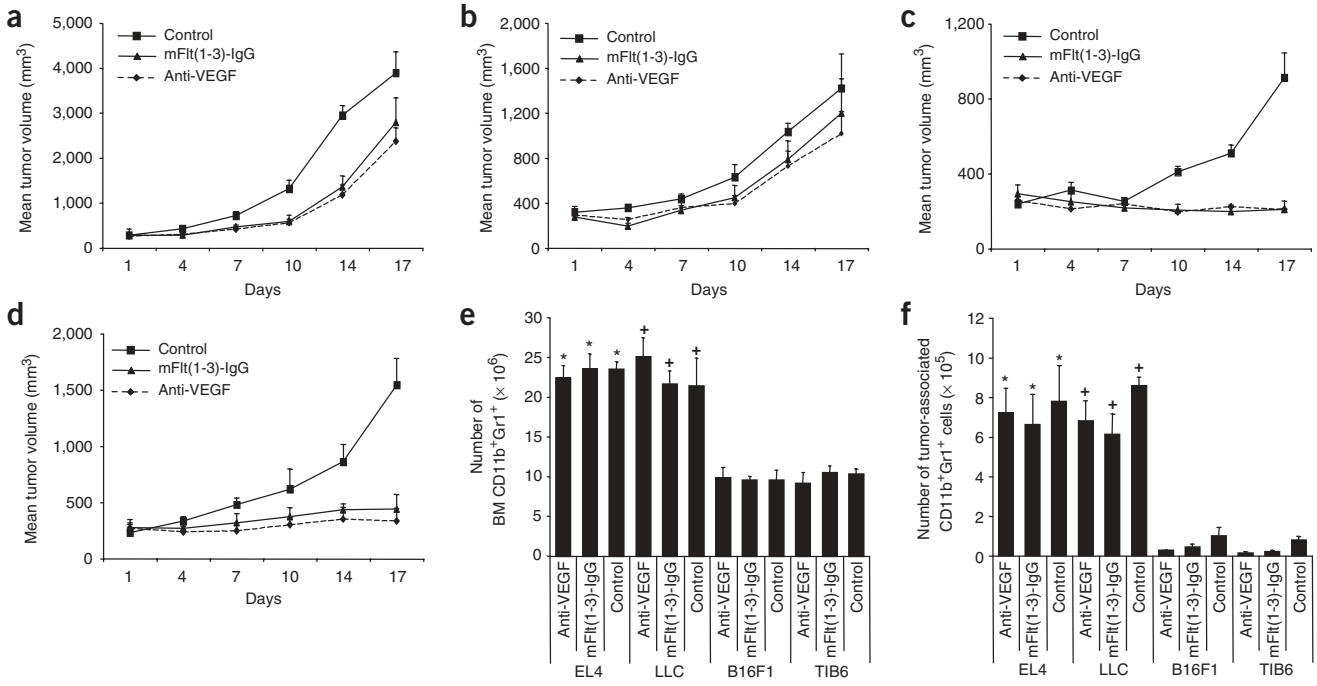

Figure 5 Comparison of the efficacy of anti-VEGF-A mAb and mFlt(1-3)-IgG in refractory and sensitive tumors. (**a**–**d**) Mice were implanted with EL4 (**a**), LLC (**b**), B16F1 (**c**) and TIB6 (**d**) tumors. Tumor-bearing mice were treated with anti-VEGF-A, mFlt(1-3)-IgG or control antibodies as described. Graphs represent mean tumor volume ± s.e.m. (**e**,**f**) Both anti-VEGF- and mFlt(1-3)-IgG-treated tumors have the ability to recruit myeloid cells. Analysis of bone marrow– and tumor-associated myeloid cells (**e** and **f**, respectively) did not reveal any significant difference in the number of myeloid cells in anti-VEGF- versus mFlt(1-3)-IgG-treated mice, in either refractory or sensitive tumors.

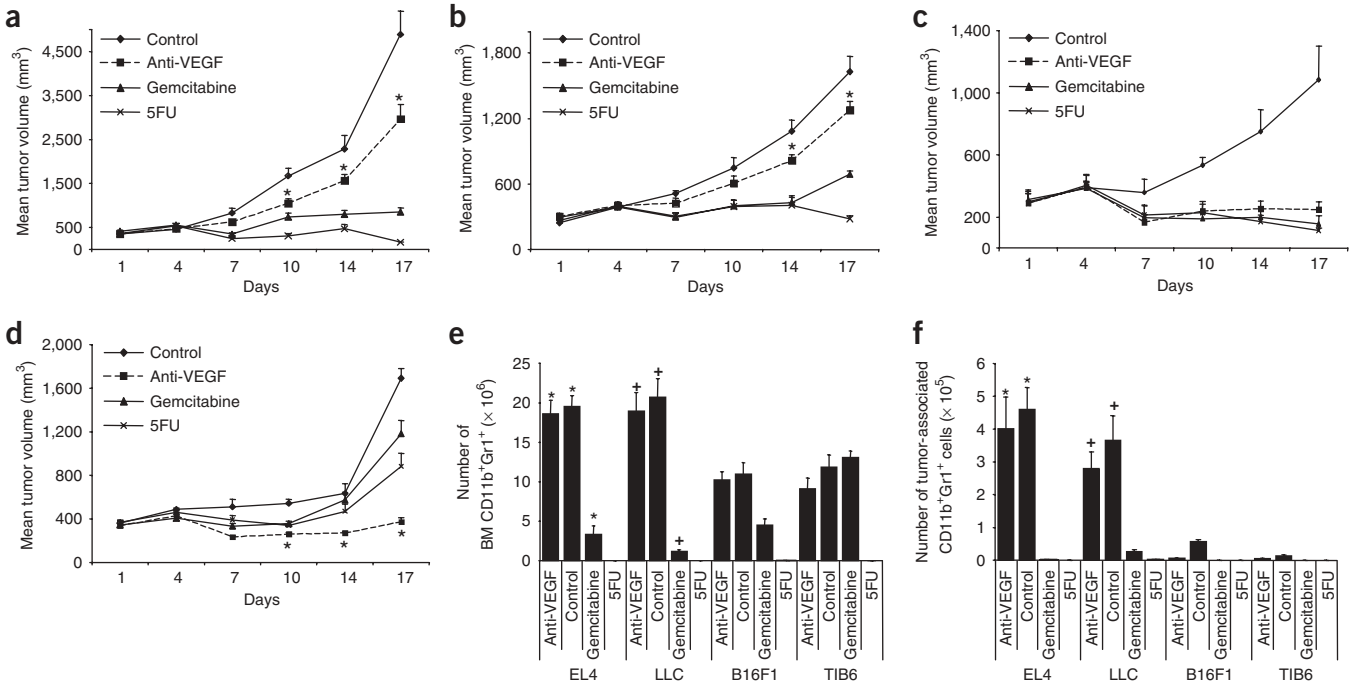

Figure 6 Distinct mechanisms mediate refractoriness to anti-VEGF and chemotherapeutic agents. (**a**–**d**) Mice ($n = 5$) were implanted with EL4 (**a**), LLC (**b**), TIB6 (**c**) and B16F1 (**d**) tumors and were then treated with anti-VEGF, control, gemcitabine or 5FU as described. Tumor volumes were measured twice weekly and all mice were analyzed at day 17. * indicates a significant difference when comparing tumors from anti-VEGF treated mice to tumors from 5FU or gemcitabine treated animals. (**e**) Bone marrow cells were isolated from each mouse and were stained with CD11b and Gr1 fluorochrome-conjugated antibodies. The graph represents the number of bone marrow $CD11b^+Gr1^+$cells in each treatment group. (**f**) Tumor isolates from each mouse were harvested after 17 d and then were stained with the same antibodies as in **e** to examine the frequency and the number of $CD11b^+Gr1^+$cells in each tumor. Bars represent mean ± s.e.m. * indicates that the difference between EL4 and B16F1 or TIB6 tumor–bearing animals is significant ($P < 0.05$). **+** indicates a significant difference between LLC ($P < 0.05$) and B16F1 or TIB6 tumor–bearing animals.

and LLC tumors showed a complete response to 5FU and a partial response to gemcitabine (**Fig. 6a**,**b**). TIB6 tumors were inhibited to a similar extent by anti-VEGF and each cytotoxic agent (**Fig. 6c**). In contrast, B16F1 tumors showed resistance to both 5FU and gemcitabine (**Fig. 6d**). These findings indicate that refractoriness to anti-VEGF does not predict resistance to chemotherapy. Interestingly, analysis of bone marrows (**Fig. 6e**) and tumors (**Fig. 6f**) showed complete ablation of $CD11b^+Gr1^+$ cells in all of the 5FU-treated mice and, to a lesser degree, in gemcitabine-treated animals. However, despite the depletion of myeloid cells in 5FU-treated mice, the growth rates of B16F1 tumors exceeded those of anti-VEGF–treated tumors, indicating that distinct mechanisms determine the refractoriness of tumors to cytotoxic agents versus anti-VEGF. Thus, refractoriness to anti-VEGF in our models does not reflect general refractoriness/resistance to anti-cancer treatments.

Distinct gene expression profile in BM $CD11b^+Gr1^+$

To gain insight into the molecular mechanisms underlying the observed functional differences among $CD11b^+Gr1^+$ cells, we compared gene expression profiles in both bone marrow and tumors between refractory and sensitive models. Unsupervised cluster analysis of gene expression in $CD11b^+Gr1^+$ cells from the bone marrow of mice primed by refractory tumors identified a distinct set of genes when compared to $CD11b^+Gr1^+$ cells from sensitive tumors (**Fig. 7a**). This suggests that, whereas major differences in gene expression exist within the primary tumors (**Supplementary Fig. 9a** online), profiles of gene expression in bone marrow myeloid cells displayed similarities among refractory tumors. Gene ontology revealed enrichment of inflammatory cytokines and markers of macrophage/myeloid cell differentiation as well as alterations in the expression of pro- and antiangiogenic factors by refractory tumors (**Fig. 7b**). Several such genes have been associated with the regulation of angiogenesis, including neurotrophin 5 (ref. 28), phospholipid scramblase (Endo-Lip)[29], angiopoietin-like 6, semaphorin VIb, Eph RA7, Eph RB2 and FGF13. Thrombospondin-1, an angiogenic inhibitor[30], was among the genes downregulated in the myeloid subset in refractory tumors. Furthermore, IL-4R[31], IL-13R[32], TLR-1R[33] and GM-CSF[34] were upregulated in bone marrow $CD11b^+Gr1^+$ cells isolated from mice bearing refractory tumors. These genes are associated with differentiation and/or activation of myeloid cells. Interestingly, several genes involved in the activation/generation of dendritic cells were markedly downregulated in bone marrow $CD11b^+Gr1^+$ cells from refractory tumors. These genes include, CD83, CD48, Crea7 and Dectin-1 (ref. 35), IL-15 (ref. 36) and CX3CR1 (ref. 37). In addition, members of the TGF-beta superfamily[38], including Smad4 and BMPR1A, are among the downregulated genes, suggesting a role for the TGF-beta pathway in regulating activation/differentiation of $CD11b^+Gr1^+$ cells in mice bearing refractory tumors. The gene expression data are also consistent with the multilineage analysis of BMMNCs (**Supplementary Fig. 5a**,**b**), showing a significant ($P < 0.05$) reduction in the frequency of $CD11c^+$ cells both in bone marrow and tumors in mice harboring refractory tumors.

Gene tree analysis in TIB6, B16F1, EL4 and LLC tumors from anti-VEGF–treated animals revealed a gene-expression profile unique to

each tumor type (**Supplementary Fig. 9a**). However, analysis of differentially expressed genes (more than twofold, $P < 0.05$) in refractory versus sensitive tumors identified several cytokines known to be involved in the mobilization of BMMNCs including granulocyte-colony stimulating factor (G-CSF)[34], and monocyte chemoattractant protein (MCP-1)[39] (**Supplementary Fig. 9b**). Furthermore, factors involved in inflammation such as macrophage inflammatory protein (MIP-2)[40] and IL-1R[41] were among the differentially expressed genes. Interestingly, several of the above cytokines (for example, G-CSF) are also known to be involved in differentiation and proliferation[42] of hematopoietic progenitors to myeloid cells. Therefore, in addition to priming and promoting mobilization of hematopoietic cells to the periphery, mice bearing refractory tumors may share the ability to stimulate myeloid cell differentiation.

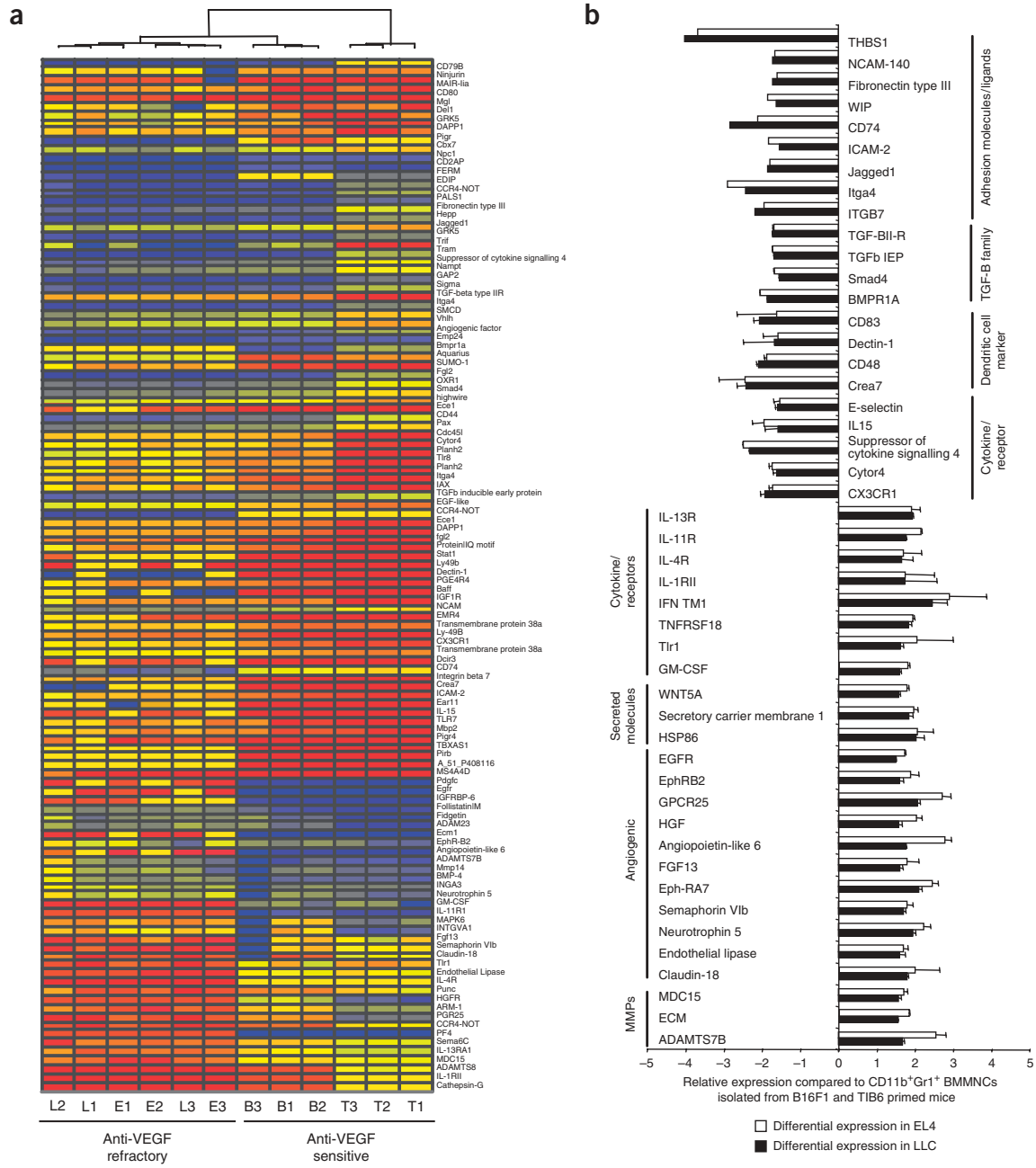

Figure 7 A distinct gene expression profile is associated with bone marrow $CD11b^+Gr1^+$ in mice bearing refractory tumors. (**a**) Gene tree analysis of $CD11b^+Gr1^+$cells isolated from the bone marrow of mice implanted with EL4 (E1-3), LLC (L1-3), B16F1 (B1-3) and TIB6 (T1-3) tumors and treated with anti-VEGF. Red and blue colors indicate up- and downregulated genes respectively. A characteristic set of changes in anti-VEGF-refractory tumors (which is different from that observed in anti-VEGF-sensitive tumors) can be identified. (**b**) Array analysis of differentially expressed genes in bone marrow $CD11b^+Gr1^+$cells isolated from mice bearing TIB6, B16F1, EL4 and LLC tumors and treated with anti-VEGF for 17 d. The graph illustrates differentially expressed genes ($P < 0.05$, > 1.5 fold) potentially involved in the regulation of angiogenesis or myeloid cell differentiation and migration, in refractory versus sensitive tumors.

In addition to the microarray analysis, we quantified the expression of a panel of factors known to be involved in angiogenesis in the tumors resulting from admixtures of B16F1 and bone marrow $CD11b^+Gr1^+$ cells. Such analysis did not reveal any distinct pattern between admixing B16F1 with bone marrow $CD11b^+Gr1^+$ cells isolated from refractory or sensitive tumors (**Supplementary Fig. 10** online). These data suggest that refractoriness to anti-VEGF treatment is unlikely to be mediated by conventional mediators of angiogenesis and novel factors or pathways may be implicated.

DISCUSSION

We show that recruitment of $CD11b^+Gr1^+$cells represents an important cellular mechanism underlying refractoriness to anti-VEGF therapy. We found that some tumors are able to recruit myeloid cells inherently and independent of treatment. However, it is possible that in other animal models of cancer or in certain circumstances, tumors may show resistance to anti-VEGF by acquiring the ability to recruit myeloid cells. Our data therefore suggest therapeutic regimens combining VEGF inhibitors with agents interfering with myeloid cell functions. Selective blockade of myeloid cell chemo-attractants would be preferable to a global myeloablation strategy, which may result in prolonged suppression of innate immunity.

Bevacizumab has significant single-agent activity in renal and ovarian carcinoma patients[43]. However, combination with cytotoxic agents had yielded the most promising therapeutic results[43]. The molecular and cellular events responsible for the increased therapeutic benefits resulting from combination treatments are currently under investigation. Increased drug uptake by tumor cells as a consequence of vessel "normalization"[44] and/or interference with endothelial cell recovery after cytotoxic damage of the tumor vasculature might account for such additive effects. It is tempting to speculate that myelo-suppression associated with cytotoxic agents also contributes to such therapeutic effects. Similar to our observations in mouse tumors, a reduction in myeloid cell numbers within primary lung tumors treated with chemotherapy did correlate with increased patient survival[45]. Therefore, targeting specific subsets of myeloid cells may increase the therapeutic benefit and perhaps prevent some of the side effects of global myeloablation by cytotoxic agents.

In conclusion, our studies identify potential cellular and molecular mechanisms mediating refractoriness to anti-VEGF therapy. Future studies will focus on the characterization of target molecules identified in the gene array analysis, their contribution to tumor expansion and specifically to refractoriness to anti-VEGF therapy.

METHODS

Cell lines. The EL4, LLC, B16F1 and TIB6 tumor cell lines were obtained from the American Type Culture Collection (ATCC) and cultured in high-glucose Dulbecco's Modified Medium (DMEM) supplemented with 10% FBS and 2 mM glutamine.

Inhibitors. Anti-VEGF mAb G6.23, which was initially derived from humanized Fab phage libraries, binds to and neutralizes murine and human VEGF-A[46]. This mAb had been previously shown to potently suppress angiogenesis associated with tumor[47] and neonatal[48] growth. For administration to immunocompetent mice, full-length reverse murine chimeric antibodies were generated by grafting the VH and VL variable domains onto the constant regions of murine IgG2a. Similar to a previous study[48], mAb G6.23 was given at the dose of 10 mg/kg, IP, twice weekly, unless indicated otherwise. Isotype-matched control antibody was mouse anti-Ragweed (IgG2a) (Genentech). The anti-Gr-1 mAb (BD BioSciences) was administered at 10 mg/kg, IP, twice weekly. Tumor measurements were performed twice weekly and terminal tumor weights were determined as described below.

The mFlt(1-3)-IgG is a chimeric protein composed of the first three Ig-like domains of murine VEGFR-1 fused to a mouse Fc (γ2B)[23,24]. Earlier studies have shown that mFlt(1-3)-IgG dramatically suppresses tumor growth when administered IP to mice at 25 mg/kg/d, starting 24 h after tumor cell inoculation[49]. The same regimen was used in the present studies.

To investigate the effects of cytotoxic agents, TIB6, B16F1, EL4 or LLC cells were implanted into C57BL/6 mice. To allow tumor establishment, treatments were initiated 4 d after tumor cell inoculation. Agents tested were 5FU (American Pharmaceutical Partner; 50 mg/kg/week) and gemcitabine (Eli Lilly; 120 mg/kg, twice a week). Both agents were administered IP. Tumor volumes were measured twice weekly and were calculated as described above.

C57BL/6 GFP chimeric mouse model. C57BL/6 (6–8 weeks) and GFP transgenic mice (C57BL/6-ACTbEGFP) were obtained from Charles River Laboratories and Jackson Laboratories, respectively. GFP expression is driven by beta-actin promoter and is expressed in most cells in GFP transgenic mice[15]. C57BL/6 GFP chimeric mice were generated by lethal irradiation (1100 Gy, Cs-irradiator) of C57BL/6 mice to ablate endogenous BMMNCs in the host, followed by rescue with 5×10^6 BMMNCs isolated from GFP transgenic mice. BMMNCs were prepared as previously described[50]. All tumor implantation experiments in chimeric mice were performed 4 weeks after hematopoietic reconstitution. For tumor growth experiments, each cell line was injected subcutaneously in the dorsal flank area. For experiments in XID mice, 1×10^7 LLC or EL4 cells were implanted.

B16F1 admixing experiments. Tumor growth studies were performed in C57BL/6 mice, GFP bone marrow chimeric mice and beige nude XID or 5×10^6 or 10^7 tumor cells (as indicated) were resuspended in 200 µl of Matrigel (Growth Factor reduced) and injected subcutaneously in the dorsal flank of mice. For B16F1 admixing experiments, BMMNCs (whole bone marrow or $CD11b^+Gr1^+$) or GFP^+ tumor–associated cells (all GFP^+ or $GFP^+CD11b^+Gr1^+$) were isolated, mixed with B16F1 cells in 200 µl Matrigel (BD BioSciences) and were implanted in the flank of C57BL/6 mice. Anti-VEGF or control treatment was initiated 4 d after tumor cell inoculation to allow the establishment of bone marrow-tumor crosstalk. Tumor size was assessed using Vernier calipers 2–3 times per week after tumors reached a palpable size. Tumor volume was determined using the $Pi/6 \times L \times W \times W$ formula with L as the longest diameter and W the diameter at the position perpendicular to L.

Immunohistochemistry. Tumor samples were frozen in Optimum Cutting Temperature (OCT, Sakura Finetek) medium, were cut (6 µm) in a cryostat (Leica Microsystem) and were frozen at –20 °C. For IHC staining, sections were dried at 20 °C for 1 h and then fixed in acetone for 10 min at –20 °C. After air-drying for 4 min at 20 °C, the nonspecific binding sites were blocked by incubation for 1 h at 20 °C in 20% normal goat serum (GIBCO BRL). Sections were stained sequentially with the following antibodies diluted in DAKO Block solution (DakoCytomation): rabbit anti-GFP AlexaFluor 488 conjugate (Molecular Probes), 20 µg/ml, for 1 h at 20 °C, goat anti-rabbit AlexaFluor 488 conjugate, 1:500 dilution for 1 h at 20 °C, rat anti-mouse PECAM-1 (Clone MEC13.3; BD Pharmingen) at 1:100 dilution overnight at 4 °C, and goat anti-rat AlexaFluor 594 conjugate (Molecular Probes), 1:500 dilution for 1 h at 20 °C. The slides were washed and mounted in DAKO fluorescent mounting medium, and immunofluorescence images were collected on an AxioPhot microscope equipped with a Plan-Apochromat 20 × objective and digitally merged.

VSA measurement. Tumor VSA was quantified from digital images of CD31-stained sections using a 20 × objective. The pixels corresponding to stained vessels were selected by using ImageJ Software, using a predetermined threshold set at 50–70 as cutoff. Contaminating (non-vessel) stray pixels were eliminated. Unless indicated otherwise, a total of 3–5 tumors per group were analyzed. A total of 15 images were taken from each tumor section, covering an area of 1,502 μm^2. Unless indicated otherwise, background staining of each group was determined by using a labeled control antibody and subtracted from the total vessel counts. The aggregate pixel vessel area, relative to the total picture area and total area analyzed, is reported as % vessel/surface area.

Flow cytometry. Tumors from control- and anti-VEGF–treated mice were isolated and single cell suspensions were obtained by mincing tumors with razor blades and homogenizing by mechanical disruption. BMMNCs were flushed from femur and tibia of implanted animals and red blood cells were lysed using ACK lysis buffer (Cambrex). Peripheral blood was collected by retro-orbital bleed and 40 µl of peripheral blood was pretreated with ACK buffer for red blood cells lysis.

Cells from bone marrow, tumor or peripheral blood were stained with a series of mAbs, specific for CD11b, Gr1, CD19, CD90, VEGFR2 (all from BD BioSciences), VEGFR1 (R&D), along with isotype-matched control to investigate the myeloid and lymphoid fractions in each compartment. FACS data were acquired on FACScalibur and analyzed by Cell Quest Pro software (BD Biosciences).

To isolate GFP$^+$ cells, single-cell suspensions were obtained from the bone marrow or tumors of implanted mice and were stained with anti-CD11b conjugated to APC and anti-Gr1 conjugated to PE. Populations of CD11b$^+$Gr1$^+$and CD11b$^-$Gr1$^-$ cells were isolated in a FACS Vantage machine and post-sort analysis ensured the purity of the population of interest in each compartment.

Cell migration assay. Tumor cells were isolated from tumor-bearing mice (day 14 after implantation) as described for FACS analysis and plated at the density of 1×10^6 cells/ml in DMEM, 10% FCS and 4 mM glutamine. After 4 d in a tissue culture incubator (5% CO_2), soluble extracts (conditioned medium) from each cell line were concentrated using Amicon spin columns (Millipore, M.W cutoff 10 kDa). For migration assay, 600 µl of triplicate samples were added to the bottom wells in transwell cell migration plates (Corning). *De novo* isolated BMMNCs (2.5×10^4) from C57BL/6 mice were resuspended in DMEM and were placed on the top chamber of the transwells. Plates were incubated at 37 °C for 9 h and migration capacity was measured by counting BMMNCs in the bottom chamber.

Microarray. RNA from bone marrow CD11b$^+$Gr1$^+$ cells was isolated using Qiagen Rneasy kit (Qiagen). Complementary RNA (cRNA) preparation and hybridization/scanning of the arrays were performed using protocols provided by Affymetrix. Briefly, five µg of total RNA was converted into double-stranded cDNA using a cDNA synthesis kit (SuperScript Choice, GIBCO/BRL) and a T7-$(dT)_{24}$ oligomer primer (Biosearch Technologies, Custom Synthesis). Double-stranded cDNA was purified on an affinity resin (Sample Cleanup Module Kit, Affymetrix) and by ethanol precipitation. After second-strand synthesis, labeled cRNA was generated from the cDNA sample using a T7 RNA polymerase and biotin-labeled nucleotide in an *in vitro* transcription reaction (Enzo Biochem). The labeled cRNA was purified on an affinity resin. The amount of labeled cRNA was determined by measuring absorbance at 260 nm and using the convention that 1 OD at 260 nm corresponds to 40 µg/ml of RNA. Twenty µg of cRNA was fragmented by incubating at 94 °C for 30 min in 40 mM Tris-acetate (pH 8.1), 100 mM potassium acetate and 30 mM magnesium acetate. Samples were then hybridized to Whole Mouse Genome 430 2.0 arrays at 45 °C for 19 h in a rotisserie oven set at 60 r.p.m. Arrays were washed, stained and scanned in the Affymetrix Fluidics station and scanner. Data analysis was performed using Spotfire software. Next, genes that were significantly ($P < 0.05$) differentially (more than 1.5-fold in CD11b analysis and more than twofold in tumor analysis) expressed in EL4 and LLC samples compared to the corresponding TIB6 and B16F1 group were selected for final analysis. Hierarchical gene cluster analysis was performed on all tumor and CD11b data using algorithms in Spotfire (Spotfire) software.

Real-time RT PCR. Total RNA was extracted from tumors using the RNeasy Mini Kit (Qiagen) along with on-column DNAseI digestion. For Taqman analysis, 100 ng of the total RNA was used per reaction. Experiments were performed in optical 96-well reaction plate and on a 9600 Emulation mode of 7500 Real time PCR machine (Applied Biosystems) using protocols provided by the manufacturer. The expression level of each gene (sequence primers are in **Supplementary Table 1** online) was further quantified against the house-keeping gene GAPDH in the same sample as described[49]. PCR conditions contained 30 min at 48 °C, 10 min at 95 °C, and 40 cycles of 15 s at 95 °C and of 60 s at 60 °C. Samples were prepared from the pool of five samples for each treatment and were run in triplicate.

Statistics. Student's *t*-test was used to determine significant differences in all experiments. A *P* value of ≤ 0.05 was considered significant.

Note: Supplementary information is available on the Nature Biotechnology website.

ACKNOWLEDGMENTS

We thank Leo DeGuzman and Jose Zavala-Solario for their help with animal experiments, Jim Cupp, Laurie Gilmour and Mike Hamilton for FACS advice and Josh Kaminker for help with the gene expression analysis.

AUTHOR CONTRIBUTIONS

F.S., H.-P.G. and N.F. designed the experiments and wrote the manuscript. F.S. analyzed the data and performed experiments. F.S., X.W., A.K.M., C.Z., M.E.B. and S.S. performed experiments. G.F. provided reagents. H.-P.G. and N.F. are both senior authors.

COMPETING INTERESTS STATEMENT

The authors declare competing financial interests: details accompany the full-text HTML version of the paper at http://www.nature.com/naturebiotechnology/.

Published online at http://www.nature.com/naturebiotechnology/
Reprints and permissions information is available online at http://npg.nature.com/reprintsandpermissions

1. Longley, D.B. & Johnston, P.G. Molecular mechanisms of drug resistance. *J. Pathol.* **205**, 275–292 (2005).
2. Hida, K. *et al.* Tumor-associated endothelial cells with cytogenetic abnormalities. *Cancer Res.* **64**, 8249–8255 (2004).
3. Pelham, R.J. *et al.* Identification of alterations in DNA copy number in host stromal cells during tumor progression. *Proc. Natl. Acad. Sci. USA* **103**, 19848–19853 (2006).
4. Ferrara, N., Gerber, H.P. & LeCouter, J. The biology of VEGF and its receptors. *Nat. Med.* **9**, 669–676 (2003).
5. Ferrara, N. Vascular endothelial growth factor: basic science and clinical progress. *Endocr. Rev.* **25**, 581–611 (2004).
6. Gerber, H.P. & Ferrara, N. Pharmacology and pharmacodynamics of bevacizumab as monotherapy or in combination with cytotoxic therapy in preclinical studies. *Cancer Res.* **65**, 671–680 (2005).
7. Casanovas, O., Hicklin, D.J., Bergers, G. & Hanahan, D. Drug resistance by evasion of antiangiogenic targeting of VEGF signaling in late-stage pancreatic islet tumors. *Cancer Cell* **8**, 299–309 (2005).
8. Kerbel, R.S. *et al.* Possible mechanisms of acquired resistance to anti-angiogenic drugs: implications for the use of combination therapy approaches. *Cancer Metastasis Rev.* **20**, 79–86 (2001).
9. Orimo, A. *et al.* Stromal fibroblasts present in invasive human breast carcinomas promote tumor growth and angiogenesis through elevated SDF-1/CXCL12 secretion. *Cell* **121**, 335–348 (2005).
10. Albini, A., Tosetti, F., Benelli, R. & Noonan, D.M. Tumor inflammatory angiogenesis and its chemoprevention. *Cancer Res.* **65**, 10637–10641 (2005).
11. Wald, M. *et al.* Mixture of trypsin, chymotrypsin and papain reduces formation of metastases and extends survival time of C57Bl6 mice with syngeneic melanoma B16. *Cancer Chemother. Pharmacol.* **47** Suppl, S16–S22 (2001).
12. Ho, R.L. *et al.* Immunological responses critical to the therapeutic effects of adriamycin plus interleukin 2 in C57BL/6 mice bearing syngeneic EL4 lymphoma. *Oncol. Res.* **5**, 363–372 (1993).
13. Liu, Y., Zhang, W., Chan, T., Saxena, A. & Xiang, J. Engineered fusion hybrid vaccine of IL-4 gene-modified myeloma and relative mature dendritic cells enhances antitumor immunity. *Leuk. Res.* **26**, 757–763 (2002).
14. Bobek, V. *et al.* Syngeneic lymph-node-targeting model of green fluorescent protein-expressing Lewis lung carcinoma. *Clin. Exp. Metastasis* **21**, 705–708 (2004).
15. Okabe, M., Ikawa, M., Kominami, K., Nakanishi, T. & Nishimune, Y. 'Green mice' as a source of ubiquitous green cells. *FEBS Lett.* **407**, 313–319 (1997).
16. Lyden, D. *et al.* Impaired recruitment of bone-marrow-derived endothelial and hematopoietic precursor cells blocks tumor angiogenesis and growth. *Nat. Med.* **7**, 1194–1201 (2001).
17. Yang, L. *et al.* Expansion of myeloid immune suppressor Gr+CD11b+ cells in tumor-bearing host directly promotes tumor angiogenesis. *Cancer Cell* **6**, 409–421 (2004).
18. Morrison, S.J., Uchida, N. & Weissman, I.L. The biology of hematopoietic stem cells. *Annu. Rev. Cell Dev. Biol.* **11**, 35–71 (1995).
19. Onai, N. *et al.* Impairment of lymphopoiesis and myelopoiesis in mice reconstituted with bone marrow-hematopoietic progenitor cells expressing SDF-1-intrakine. *Blood* **96**, 2074–2080 (2000).
20. Kusmartsev, S. & Gabrilovich, D.I. Immature myeloid cells and cancer-associated immune suppression. *Cancer Immunol. Immunother.* **51**, 293–298 (2002).
21. Bronte, V. *et al.* Identification of a CD11b(+)/Gr-1(+)/CD31(+) myeloid progenitor capable of activating or suppressing CD8(+) T cells. *Blood* **96**, 3838–3846 (2000).

22. Hestdal, K. *et al.* Characterization and regulation of RB6–8C5 antigen expression on murine bone marrow cells. *J. Immunol.* **147**, 22–28 (1991).
23. Davis-Smyth, T., Chen, H., Park, J., Presta, L.G. & Ferrara, N. The second immunoglobulin-like domain of the VEGF tyrosine kinase receptor Flt-1 determines ligand binding and may initiate a signal transduction cascade. *EMBO J.* **15**, 4919–4927 (1996).
24. Ferrara, N. *et al.* Vascular endothelial growth factor is essential for corpus luteum angiogenesis. *Nat. Med.* **4**, 336–340 (1998).
25. Holash, J. *et al.* VEGF-Trap: a VEGF blocker with potent antitumor effects. *Proc. Natl. Acad. Sci. USA* **99**, 11393–11398 (2002).
26. Barleon, B. *et al.* Migration of human monocytes in response to vascular endothelial growth factor (VEGF) is mediated via the VEGF receptor flt-1. *Blood* **87**, 3336–3343 (1996).
27. Hattori, K. *et al.* Placental growth factor reconstitutes hematopoiesis by recruiting VEGFR1(+) stem cells from bone-marrow microenvironment. *Nat. Med.* **8**, 841–849 (2002).
28. Lazarovici, P., Gazit, A., Staniszewska, I., Marcinkiewicz, C. & Lelkes, P.I. Nerve growth factor (NGF) promotes angiogenesis in the quail chorioallantoic membrane. *Endothelium* **13**, 51–59 (2006).
29. Favre, C.J. *et al.* Expression of genes involved in vascular development and angiogenesis in endothelial cells of adult lung. *Am. J. Physiol. Heart Circ. Physiol.* **285**, H1917–H1938 (2003).
30. Good, D.J. *et al.* A tumor suppressor-dependent inhibitor of angiogenesis is immunologically and functionally indistinguishable from a fragment of thrombospondin. *Proc. Natl. Acad. Sci. USA* **87**, 6624–6628 (1990).
31. Palmer-Crocker, R.L., Hughes, C.C. & Pober, J.S. IL-4 and IL-13 activate the JAK2 tyrosine kinase and Stat6 in cultured human vascular endothelial cells through a common pathway that does not involve the gamma c chain. *J. Clin. Invest.* **98**, 604–609 (1996).
32. Roy, B. *et al.* IL-13 signal transduction in human monocytes: phosphorylation of receptor components, association with Jaks, and phosphorylation/activation of Stats. *J. Leukoc. Biol.* **72**, 580–589 (2002).
33. Edfeldt, K., Swedenborg, J., Hansson, G.K. & Yan, Z.Q. Expression of toll-like receptors in human atherosclerotic lesions: a possible pathway for plaque activation. *Circulation* **105**, 1158–1161 (2002).
34. Rapoport, A.P., Abboud, C.N. & DiPersio, J.F. Granulocyte-macrophage colony-stimulating factor (GM-CSF) and granulocyte colony-stimulating factor (G-CSF): receptor biology, signal transduction, and neutrophil activation. *Blood Rev.* **6**, 43–57 (1992).
35. Lechmann, M., Berchtold, S., Hauber, J. & Steinkasserer, A. CD83 on dendritic cells: more than just a marker for maturation. *Trends Immunol.* **23**, 273–275 (2002).
36. Feau, S. *et al.* Dendritic cell-derived IL-2 production is regulated by IL-15 in humans and in mice. *Blood* **105**, 697–702 (2005).
37. Niess, J.H. *et al.* CX3CR1-mediated dendritic cell access to the intestinal lumen and bacterial clearance. *Science* **307**, 254–258 (2005).
38. Derynck, R., Akhurst, R.J. & Balmain, A. TGF-beta signaling in tumor suppression and cancer progression. *Nat. Genet.* **29**, 117–129 (2001).
39. Leonard, E.J., Skeel, A., Yoshimura, T. & Rankin, J. Secretion of monocyte chemoattractant protein-1 (MCP-1) by human mononuclear phagocytes. *Adv. Exp. Med. Biol.* **351**, 55–64 (1993).
40. Cook, D.N. The role of MIP-1 alpha in inflammation and hematopoiesis. *J. Leukoc. Biol.* **59**, 61–66 (1996).
41. Dinarello, C.A. Blocking IL-1 in systemic inflammation. *J. Exp. Med.* **201**, 1355–1359 (2005).
42. Lemoli, R.M. *et al.* Proliferative response of human acute myeloid leukemia cells and normal marrow enriched progenitor cells to human recombinant growth factors IL-3, GM-CSF and G-CSF alone and in combination. *Leukemia* **5**, 386–391 (1991).
43. Ferrara, N., Hillan, K.J., Gerber, H.P. & Novotny, W. Discovery and development of bevacizumab, an anti-VEGF antibody for treating cancer. *Nat. Rev. Drug Discov.* **3**, 391–400 (2004).
44. Jain, R.K. Normalizing tumor vasculature with anti-angiogenic therapy: a new paradigm for combination therapy. *Nat. Med.* **7**, 987–989 (2001).
45. Di Maio, M. *et al.* Chemotherapy-induced neutropenia and treatment efficacy in advanced non-small-cell lung cancer: a pooled analysis of three randomised trials. *Lancet Oncol.* **6**, 669–677 (2005).
46. Liang, W.C. *et al.* Cross-species VEGF-blocking antibodies completely inhibit the growth of human tumor xenografts and measure the contribution of stromal vegf. *J. Biol. Chem.* **281**, 951–961 (2006).
47. Dong, J. *et al.* VEGF-null cells require PDGFR alpha signaling-mediated stromal fibroblast recruitment for tumorigenesis. *EMBO J.* **23**, 2800–2810 (2004).
48. Malik, A.K. *et al.* Redundant roles of VEGF-B and PlGF during selective VEGF-A blockade in mice. *Blood* **107**, 550–557 (2006).
49. Gerber, H.P., Kowalski, J., Sherman, D., Eberhard, D.A. & Ferrara, N. Complete inhibition of rhabdomyosarcoma xenograft growth and neovascularization requires blockade of both tumor and host vascular endothelial growth factor. *Cancer Res.* **60**, 6253–6258 (2000).
50. Gerber, H.P. *et al.* VEGF regulates haematopoietic stem cell survival by an internal autocrine loop mechanism. *Nature* **417**, 954–958 (2002).